forum acusticum 2026
8-12 September · Graz, Austria

SENSITIVITY STUDY OF MEASUREMENTS PROCEDURE AND PARAMETERS IN EXPERIMENTAL MODAL ANALYSIS OF CERAMIC COMPONENTS

Michał Kozupa[1], Jadwiga Hyla[1]
[1]*Hitachi Energy Research*
Pawia 7, 31-154 Krakow,
Poland

This paper is a revised version of the authors' submitted manuscript that was peer-reviewed by at least two anonymous reviewers.

Abstract

This work presents a comprehensive sensitivity study on the influence of measurement procedures and parameters in the experimental modal analysis (EMA) of ceramic blocks, with a focus on optimizing the identification of resonance frequencies and damping ratios for ceramic components used in power products applications. The study systematically investigates how variations in sample mounting, actuator placement, mesh density, and measurement settings affect the accuracy and reliability of modal parameters.

A series of preliminary tests were conducted to evaluate the impact of actuator orientation and distance from the sample edge, revealing that while global actuator position has negligible effect on resonance frequencies, proximity to the edge significantly enhances dynamic response. The measurement methodology was further refined by analyzing the effects of mesh density on frequency and mode shape identification.

Across a range of sample thicknesses, this study identifies trends in resonance frequency shifts and damping values, providing insights into the relationship between geometric parameters and modal behavior. The findings underscore the critical role of measurement procedure optimization in achieving accurate EMA results and offer guidance for future experimental campaigns and numerical model development.

Keywords: *experimental modal analysis, measurement procedure, laser Doppler vibrometry, sensitivity study*

1. Introduction

Experimental modal analysis (EMA) is widely used to determine vibrational characteristics of structures and is particularly important for brittle ceramic components in power equipment. Because of their high stiffness and low damping, ceramic materials exhibit sharp resonance peaks that are highly sensitive to test conditions. Recent studies have shown that variations in test procedures and parameters can significantly influence modal results. For example, inadequate free-free support during testing can effectively stiffen the structure, thereby introducing errors in the measured natural frequencies and damping values [1]. Similarly, suboptimal excitation or sensor placement can hinder full mode identification by failing to excite or capture certain modes [2]. A recent EMA study on ceramic masonry confirmed that even subtle changes (such as damage-induced stiffness loss) produce detectable shifts in modal parameters, underscoring the technique's sensitivity and the need for rigorous test setups [3]. However, a comprehensive multi-parameter sensitivity analysis specific to ceramic EMA remains lacking. This paper addresses that gap by investigating how variations in sample mounting, exciter placement, and measurement resolution affect the identified modal parameters of ceramic samples, with the goal of establishing guidelines for robust EMA of ceramics and ensuring reliable modal data for design and material evaluation.

2. Description of tested samples

The specimens analyzed in this work were technical ceramic blocks (disc-shaped insulators) made of an isotropic steatite ceramic. Each sample was an oval/circular plate-like ceramic block with a nominally uniform cross-section. To investigate the effect of geometry on modal behavior, the test samples covered a range of thicknesses. Four representative thicknesses were selected for the first series of specimens: 6.5 mm, 9.5 mm, 21.2 mm, and 34.1 mm. All samples in this series had the same in-plane shape (approximately circular with a diameter of about 100 mm) and material composition, differing only in thickness; this choice of samples allowed observation of how increasing thickness shifts the resonant frequencies.

3. Measurement methodology

Vibration measurements at points on the tested samples were conducted in one dimension (1D) using a PSV laser vibrometer equipped with the main scanning head. The laser vibrometer head was positioned parallel to the axis of the tested element. Additionally, the following equipment was used for the measurements:

- Falco-Systems WMA-300 High-Speed High-Voltage Amplifier,
- ThorLabs PA25FEW Round Piezoelectric Chip with Wires, Ø5.0 mm.

The actuator was glued with the cyanoacrylate adhesive, with its orientation on the sample being variable. Each tested sample was freely suspended in air using elastic bands, tape, and cyanoacrylate adhesive, as shown in Fig. 1. These measures were taken to replicate free-free boundary conditions during testing.

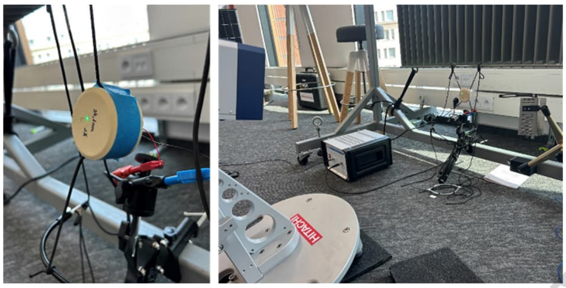

Figure 1. Measurement setup.

The voltage applied to the actuator was consistent with the measurement settings and was further amplified by a factor of 50, resulting in a 40 V output at the actuator. The Table 1 presents detailed information on the measurement settings, including frequency range, overlap, and the number of averages:

Table 1. LDV Measurement settings.

Acquisition mode:	FFT
Data averaging type:	Complex (Magnitude, Phase)
Averaging Count:	15
Window:	Rectangle
Frequency Bandwidth:	100 kHz, from 5 kHz to 100 kHz
FFT Lines:	102400
Overlap:	25%
Sample Frequency:	250 kHz
Sample Time:	1.024 s
Resolution:	976.5625 mHz
Function generator signal:	Periodic Chirp
Signal amplitude:	800 mV

The measurement grid for each sample was similar in structure and consisted of approximately 100 measurement points. Point density was increased in the central region of the sample, while it was intentionally reduced in the peripheral areas. The base grid layout was defined as circular. An example of the measurement grid configuration is shown in the Fig. 2.

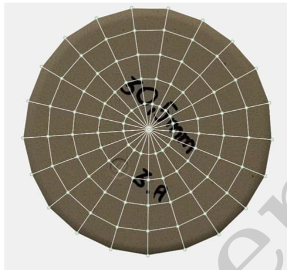

Figure 2. Example of measuring grid.

4. Preliminary measurements

Prior to the main measurement session, a series of tests were conducted to evaluate the influence of actuator placement on the sample. The session was divided into two stages: global placement of the actuator at various positions across the sample surface and placement of the actuator at a defined distance from the sample edge. A sample with a thickness of 6.5 mm was used for these measurements. The preliminary analysis enabled the most accurate possible measurements to be performed on the remaining samples.

4.1 Impact of sample mounting orientation

Initially, a study was conducted to verify the influence of the boundary conditions change reflected in rotating the measurement sample. The actuator was fixed in a single location, and measurements were performed in three different orientations, looking at back: top-left corner of the sample, top-right corner, and the bottom-central region. The actuator's position was altered by changing the mounting orientation of the sample , as shown in Fig. 3. In all cases, the free boundary conditions were applied.

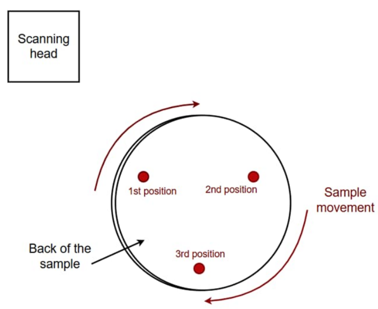

Figure 3. Tested exciter positions scheme.

Based on the results obtained, no influence of rotating the sample thus slightly changing boundary conditions and sample fixation on the frequency response function (FRF) of the tested sample was observed. The resonance frequencies remained highly consistent across all configurations , as shown in Table 2. Detailed statistical analysis showed that the highest standard deviation occurred for the 5th and 6th modes, reaching approximately 100 Hz. For the remaining results, the standard deviation values were minor and negligible—typically not exceeding 50 Hz. For each sample position, the resonance frequencies were clearly identifiable, as shown in Fig. 4, and determining the 3 dB drop—required for further analysis—was straightforward. At this stage, the exact values of the modal frequencies were not subject to detailed analysis. This test proved that for the following measurement campaign of other samples there is no meaningful influence of the mounting as well as the sample positioning.

Table 2. First ten modes' values and basic statistics.

no.	Frequency, kHz						
	1st position	2nd position	3rd position	mean	std	min	max
1	11.4	11.3	11.4	11.4	0.04	11.3	11.4
2	17.8	17.8	17.8	17.8	0.02	17.8	17.8
3	25.0	24.9	25.0	25.0	0.05	24.9	25.0
4	38.0	38.0	38.1	38.0	0.04	38.0	38.1
5	41.1	41.1	41.3	41.2	0.10	41.1	41.3
6	50.3	50.0	50.1	50.2	0.14	50.0	50.3
7	57.3	57.2	57.2	57.3	0.02	57.2	57.3
8	59.3	59.2	59.4	59.3	0.07	59.2	59.4
9	60.6	60.4	60.6	60.5	0.07	60.4	60.6
10	65.7	65.7	65.8	65.7	0.05	65.7	65.8

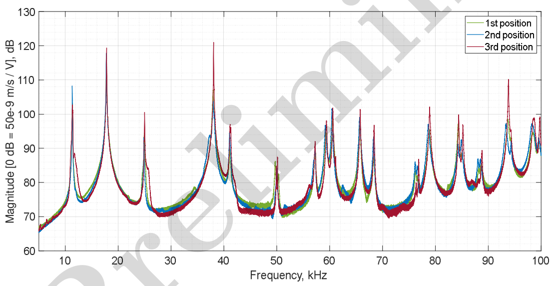

Figure 4. Comparison of FRF results for different orientation of piezo exciter.

4.2 Impact of exciter distance from sample edge

The next stage of the preliminary study involved verifying the influence of the actuator's mounting distance from the sample edge. As the sample is circular the location of the exciter should be sensitive only to one dimension – distance to the center/edge. The Fig. 5 shows three successive actuator positions: the second position was located closest to the center of the sample, the third was nearest to the edge, and the first position was intermediate, placed between the second and third. Three actuators were used for this test - each mounted sequentially at the designated positions. As in the previous stages, the sample was freely suspended during each measurement. During this session, the actuator was mounted in the bottom-central region of the sample.

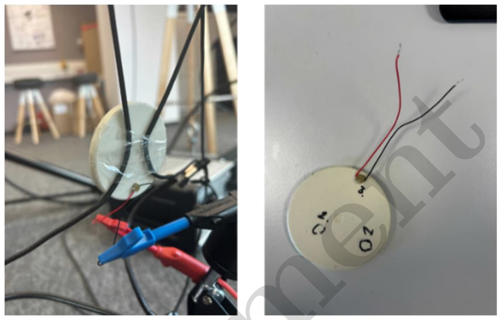

Figure 5. Tested exciter positions.

The results, placed in Table 3, indicate significant variation depending on the actuator's position. Based on Fig. 6, a noticeable difference in dynamic response was also observed depending on actuator placement, particularly at higher frequencies. The highest standard deviation was recorded for the seventh mode, reaching nearly 300 Hz and for eighth mode the high standard deviation can be observed. For the third and fourth mode, the standard deviation exceeded 100 Hz. In the remaining cases, the deviations were minor and negligible. As in the first stage of the preliminary analysis, a detailed discussion of the resonance results and modal analysis will be presented in the subsequent sections of the report.

Table 3. First ten modes' values and basic statistics.

no.	Frequency, kHz						
	1st position	2nd position	3rd position	mean	std	min	max
1	11.4	11.4	11.4	11.4	0.01	11.4	11.4
2	17.8	17.8	17.8	17.8	0.02	17.8	17.8
3	25.0	25.1	24.8	25.0	0.11	24.8	25.1
4	38.1	37.8	38.2	38.0	0.17	37.8	38.2
5	41.3	41.4	41.2	41.3	0.09	41.2	41.4
6	50.1	50.1	50.2	50.2	0.01	50.1	50.2
7	57.2	57.5	56.8	57.2	0.30	56.8	57.5
8	59.4	59.7	59.2	59.4	0.20	59.2	59.7
9	60.6	60.5	60.4	60.5	0.08	60.4	60.6
10	65.8	65.7	65.5	65.7	0.09	65.5	65.8

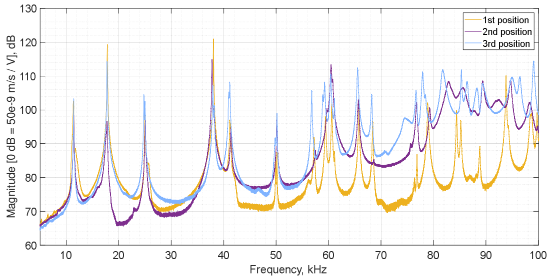

Figure 6. Comparison of FRF results for different position of piezo exciter.

4.3 Modal Assurance Criterion analysis

To ensure accurate identification of the first ten modes, a comparison was made between the mode shapes obtained from the theoretical model, shown in Fig. 7 and those derived from experimental measurements shown in Fig. 8, prior to presenting the results. This comparison was carried out using the sample with a thickness of 6.5 mm.

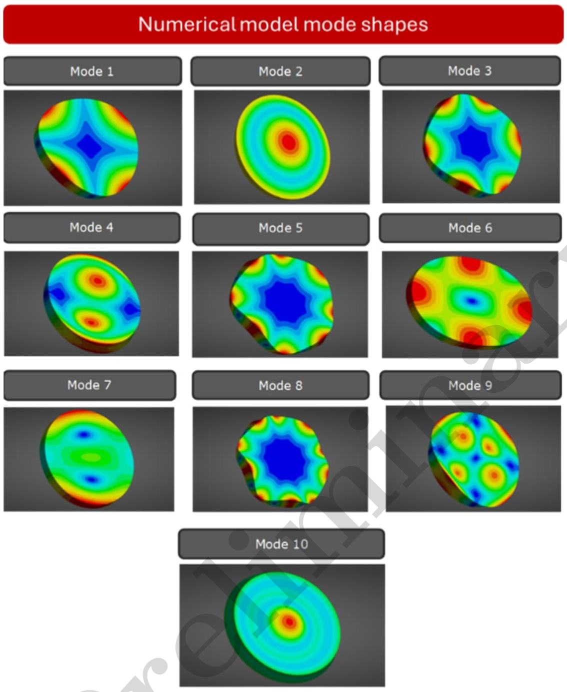

Figure 7. First ten mode shapes calculated in FEM ANSYS software.

Correct mode identification also enables precise determination of damping parameters, which will be critical in the following stages of the analysis.

The Auto MAC matrix, shown in Fig. 9, also indicates a significant similarity between mode 7 and mode 2 (approximately 30%). Additional similarities were observed between:

- mode 10 and mode 2,
- mode 7 and mode 1,
- mode 10 and mode 7 (each around 20%).

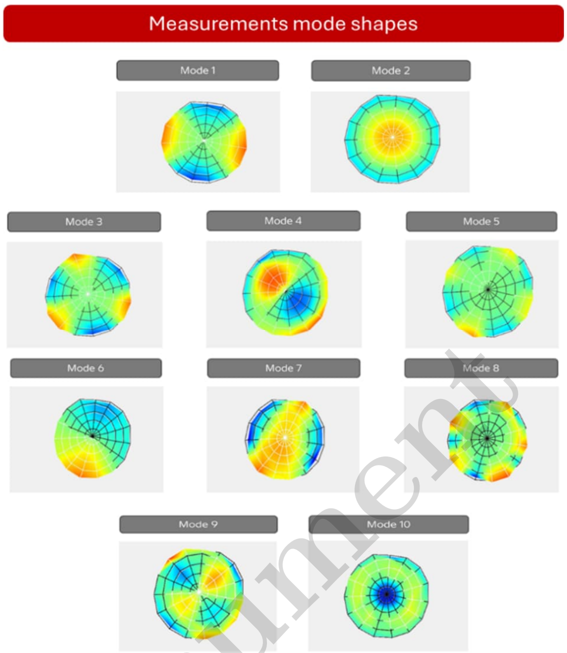

Figure 8. First ten mode shapes from measurements.

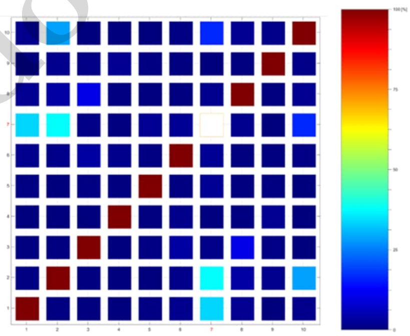

Figure 9. Auto MAC table for modal analysis calculated in Polywave software.

The measured values were compared with those obtained from the FEM model for the ceramic material. Additionally, the absolute difference, expressed as a percentage, was calculated to assess discrepancies between individual modes, as shown in Table 4. As can be observed, the differences are very small. Based on the presented data, the maximum differences are less than 2% and occur for the second, ninth, and tenth modes. The largest differences are highlighted in yellow, while the remaining values are very close to each other.

Table 4. Frequency values of first ten modes comparison for measured values and numerical model results.

Mode number	Mode shapes (diameter, circular)	Frequency, kHz		Difference , %
		Measured values	Numerical model values	
1	(2,1)	11.42	11.43	0.088
2	(0,1)	17.78	18.09	1.728
3	(3,1)	25	25.09	0.359
4	(1,2)	37.93	38.5	1.492
5	(4,1)	41.18	41.48	0.726
6	(1,1)	50.15	50.13	0.040
7	(0,2)	56.78	57.5	1.260
8	(5,1)	59.26	59.79	0.890
9	(2,2)	60.4	61.47	1.756
10	(0,3)	65.54	66.54	1.514

The Modal Assurance Criterion (MAC) analysis reveals a high level of agreement between the experimental and theoretical mode shapes for the first five modes, with MAC values exceeding 0.6, as shown in Fig. 10. A renewed correlation is also observed for the last three modes, although the MAC value for mode 9 is slightly lower.

The greatest discrepancies are found in modes 6 and 7, where—highlighted in red—no significant similarity is observed. An interesting observation is the similarity between mode 6 from the measurement and mode 7 from the theoretical model. However, mode 7 from the measurement does not show meaningful correlation with any of the theoretical modes.

Additional cross-correlations between modes include:

- Measured mode 1 and theoretical mode 6,
- Measured mode 2 and theoretical mode 10,
- Theoretical mode 2 and measured mode 7

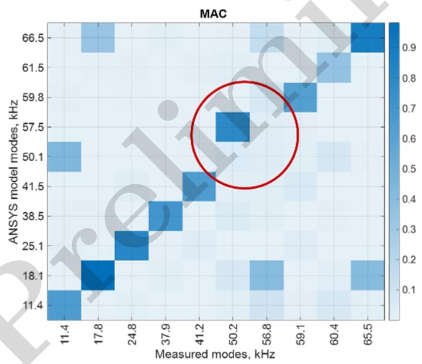

Figure 10. Modal Assurance Criterion analysis for measured and ANSYS model results.

To extend the analysis, a comparison of the computed modal parameters in ANSYS was presented for the considered case. The evaluation included two clearly matching cases and one instance of mode shift between the experimental measurement and the theoretical value calculated in ANSYS.

For mode 2, the MAC matrix indicates a clear agreement—both the experimental and theoretical results correspond to mode (0,1). The only difference lies in the frequency, which varies by approximately 300 Hz between the two cases. For comparison, mode 6 was analysed, where two distinct mode shapes were obtained at a frequency of approximately 50 kHz , as shown in Fig. 11.

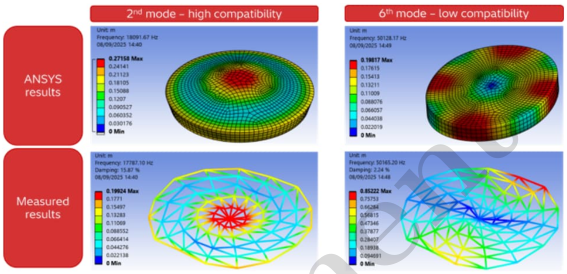

Figure 11. Ansys-Measured results comparison – unambiguous values.

5. Final results

5.1 Modal analysis

The presentation of the frequency response function (FRF) spectra was guided by the results obtained from the conducted measurements, focusing on various sample thicknesses and material types.

A comparison of the results for samples with thicknesses of 6.5 mm and 9.5 mm reveals a significant reduction in the dynamic range of the frequency response function (FRF) spectrum for the thicker sample , as shown in Fig. 12. In the case of the thinner sample, the first resonance frequency is located around 11.3 kHz, whereas for the 9.5 mm sample, the first mode appears near 16.3 kHz. In both cases, the first mode exhibits a lower amplitude than the second, which is particularly pronounced for the 9.5 mm sample. A high dynamic range of subsequent resonances is especially evident above 80 kHz for the 6.5 mm sample. For the 9.5 mm sample, it is possible to directly determine a finite number of resonance frequencies, enabling straightforward identification of successive modes. In contrast, the thinner sample requires more advanced analysis to accurately identify higher-order modes.

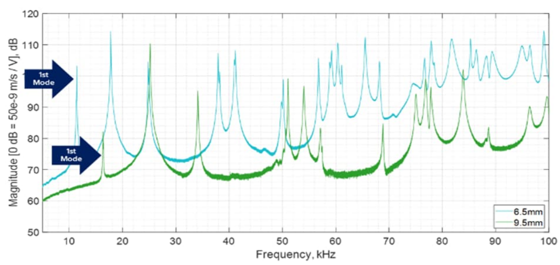

Figure 12. Comparison of FRF spectrum of thinner samples.

For significantly thicker samples, a noticeable shift of the first mode toward higher frequencies was observed. In this case, a substantially greater spectral dynamic range is evident for the sample with a thickness of 34.1 mm, as shown in Fig. 13. The first resonance frequency for the 21.2 mm sample is located slightly below 30 kHz, while for the 34.1 mm sample it exceeds 35 kHz. In both cases, the spacing between the first and second modes is approximately 10 kHz, indicating a considerably larger difference compared to thinner samples. Similar to the analysis of narrower samples, the 21.2mm sample allows for a straightforward and unambiguous identification of a finite number of resonance frequencies corresponding to successive modes. However, for the 34.1 mm sample, a more comprehensive analysis is required to accurately identify higher-order modes. Once again, a pronounced increase in dynamic range is observed above 80 kHz for the thickest sample.

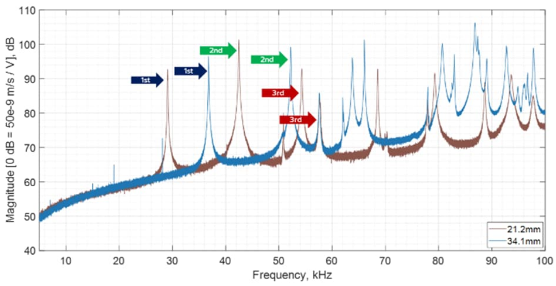

Figure 13. Comparison of FRF spectrum of thicker samples.

5.2 Damping analysis

The Table 5 presents the first ten modes for each of the analysed first series of samples, clearly showing a shift in successive resonance frequencies with increasing material thickness. Additionally, damping ratio values for each thickness group are included. The highest damping values are marked in red, while the lowest are marked in green. No consistent relationship was observed between the mode number and the corresponding damping value. The highest damping values were recorded for the thinnest sample (6.5 mm), with a maximum of 0.18% and a minimum of 0.08%. Most values for this sample exceeded 0.10%. Compared to the results for the thickest sample, the damping values across all ten modes were noticeably lower. Additionally, for thicker samples, not all the considered modes were identified. Despite the observed downward trend in damping values with increasing sample thickness, the overall values remain low, indicating prolonged oscillation before vibration decay. This behaviour is typical for materials used in systems where minimal energy loss is desired.

Table 5. Damping results for tested samples.

no.	6.5mm		9.5mm		21.2mm		34.1mm	
	fn, kHz	damping, %	fn, kHz	damping, %	fn, kHz	damping, %	fn, kHz	damping, %
1	11.42	0.15	16.33	0.16	29.08	0.12	36.79	0.10
2	17.79	0.17	25.18	0.14	42.49	0.10	52.22	0.11
3	25.00	0.18	34.13	0.16	54.31	0.14	63.79	0.13
4	38.21	0.16	51.05	0.07	68.56	0.07	86.83	0.13
5	41.18	0.13	54.01	0.15	79.27	0.16	89.04	0.10
6	50.16	0.08	57.13	0.18	97.79	0.28	94.90	0.18
7	56.78	0.10	68.85	0.10			96.73	0.09
8	59.23	0.15	75.05	0.18				
9	60.40	0.15	76.88	0.16				
10	65.54	0.14	83.91	0.14				

6. Conclusion

In this study, variations in the experimental modal analysis procedure for ceramic components were systematically examined. The results demonstrated that sample mounting orientation under free-free support has negligible effect on identified resonance frequencies, whereas the exciter's placement significantly influences higher-frequency modes (e.g. shifts of ~0.3 kHz for certain modes when the exciter is near the edge). As sample thickness increased, fundamental frequencies rose (from ~11 kHz at 6.5 mm to ~16 kHz at 9.5 mm) and damping ratios decreased (e.g. 0.15–0.18% in the thinnest vs ~0.08–0.10% in the thickest sample). Importantly, experimental modal frequencies agreed with finite element predictions within ~2%, and mode shapes showed strong correlation (MAC $>$ 0.6 for most modes). These findings validate the test methodology and highlight critical factors – especially transducer placement – for obtaining reliable EMA data to inform design and simulation of ceramic components.

References

[1] D. Jiang et al., "Reducing effects of boundary condition in modal testing of flexible structures," *J. Mech. Sci. Technol.*, vol. 38, no. 1, pp. 89–99, 2024.

[2] E. Gülbahçe and M. Çelik, "Investigation of the effect of modal analysis correlation on actuator/sensor positions for plate structures," *Vibroengineering Procedia*, vol. 43, pp. 135–142, 2022.

[3] M. Żółtowski et al., "Vibration energy signal information for measuring dynamic preferences of ceramic building materials using EMA methodology," *Materials*, vol. 15, no. 4, Art. 1452, 2022.

Corresponding author: *michal.kozupa@hitachienergy.com*